

# Solder Joints Failure Under Low Strain-rate Cyclic Loading

Jie Lian, Ph.D., Dennis Willie, Jada Chan, Francoise Sarrazin, Ph.D., Kelvin Wong, Christopher Vu, Wesley Tran, Tuyen Nguyen, Tu Tran, Anwar Mohammed, Ph.D., Michael Doiron  
FLEX International, Milpitas, CA

## Abstract

Solder joint reliability has been a key issue for electronic assemblies and microelectronic packaging for many years. Many different factors can affect the solder joint reliability, such as package construction, mechanical properties of solder joints, external mechanical and thermal stresses, and environmental change. In applications of portable electrical devices, the mechanical impact such as shock, bending and twisting plays an important role in the product's reliability. When an electronic assembly experiences repeatable mechanical stresses, failure of the solder joint may be induced. In this study, we carried out a series of experiments to understand the failure mode of Sn-Cu solder joints under mechanical bending at the product level. By comparing two different designs with button/switches, the bending induced strain was found to be the key factor that makes the solder joint fail. Low strain-rate cyclic button push tests were performed with PCB board strain measured simultaneously by strain gage. A number of analytical methods were used to study the failure modes under different button push conditions, such as dye and pry, cross section, and X-ray. The black pad defect was observed with the Electroless Nickel Immersion Gold (ENIG) surface finish between the component and board pad, which contributed to the brittle fracture in the intermetallic region. Ductile fractures were observed inside the bulk solder, which was attributed to the high strain at low strain-rate cyclic loading during operations. To eliminate the solder joint crack and improve the interconnection reliability, alternative surface finishes and methods to reduce the board strain were suggested.

**Key Words:** Cyclic bending, Black Pad, Solder Joint Failure, Strain Gage Measurement

## Introduction

Portable consumer electronics have experienced significant growth during the past few years. Recent trends of making the electronic devices lighter, thinner, and faster bring more challenges in the reliability of microelectronics packaging, assembly and testing. Among several reliability considerations in the portable consumer electronics, solder joint integrity is of great importance. Since they serve as the mechanical and electrical interconnects in a package, and failure of solder joints can fail the whole system. Various factors can affect the solder joint integrity, such as package construction, mechanical properties of solder joints, external mechanical and thermal stresses, and environmental change. In this study, failure mechanisms of SAC305 solder joints (96.5% tin, 3% silver, and 0.5% copper) on copper pad with an Electroless Nickel Immersion Gold (ENIG) surface finish were studied from field returned handheld consumer electronic devices. The objective is to find out the root cause of the failure in the returned devices, and to investigate other potential reliability risks and failure mechanisms under long term operating conditions.

Solder joints are particularly prone to failure when the product experiences some high strain-rate or high strain event, such as bending, mechanical shock or drop. By evaluating the handheld consumer products, a high extent of bending fatigue of the Ball Grid Array (BGA) package was found in operating conditions. It is thus important to understand how this bending fatigue affects the product performance, and the failure mechanisms in the Sn-Cu solder joints. To simulate the operating conditions, low strain-rate cyclic bending tests were performed on the product level. Strain gage measurement was implemented on the PCB board surrounding the BGA to understand the differences of strain between the product level bending and the board level bending, between human manual bending and a machine-controlled bending, and between two different external enclosures. The influence from strain levels and external enclosure button design were evaluated. Factors that contribute to the different failure modes were further discussed.

## Experimental

Two groups of the consumer electronic devices were used for the study. The first group (group 1) are field returned units with known failures. The second group (group 2) are the brand new functional units with two different enclosure structures. Two failed samples (sample 1 and sample 2) from group 1 were first investigated with a series of failure analysis tools. From electrical function tests, the failures were identified located in the corner sites inside the BGA package. Figure 1 shows the BGA outline drawing with numbers that identify all grid positions of the Sn-Cu solder balls. To learn about the full map of

failed solder balls, dye and pry testing was performed on the BGA package of sample 1. The BGA package was submerged into red dye, allowing the dye to penetrate any cracks or defects. Then the BGA package was mechanically separated from the PCB. Regions with red dye color indicate the presence of open circuits, fractures, or cracks. Furthermore, sample 2 was cross sectioned to reveal the failure mode. Scanning Electron Microscopy imaging coupled with Energy Dispersive X-ray Spectroscopy was taken to reveal the microstructure and composition of the solder joint in sample 2.

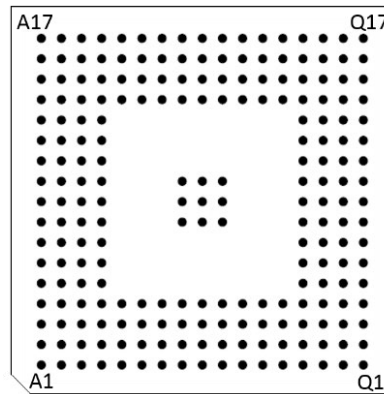


Figure 1. BGA land pattern with solder ball numbers labeled.

As consumer portable products are commonly subjected to mechanical stresses, such as bending, twisting, mechanical shock (drop), or vibration, it is necessary to evaluate the performance of the BGA under such stresses. On the other hand, the failed BGA package was known to be subjected to repeated bending induced strain because of the product structure. Thus, we would like to investigate how the repeated bending stress affects the solder joint failure, and what is the failure mechanism. Low strain-rate cyclic button push tests were performed at the product level on the 2 samples in group 2 with two different enclosure structures, that we named old design and new design. Based on past evaluations of the old design, in the new design, improvements were made by applying more constraints on PCB deformation and changing external enclosure materials to lower the switch activation stress. The strain changes were simultaneously measured by installing strain gages on the board at the corners of the BGA. The strain was measured for two purposes. First is to check whether the strain of the BGA meet IPC/JEDEC-9704 standard for strain limits, and second is to compare the strain differences at the product level and the board level during operation, with the old design and the new design. Thus, evaluation on the impact of the enclosure design on strain variations can be achieved. Figure 2 shows the setup for the low strain-rate cyclic button push tests. It consists of a mechanical tester for button push tests, and a strain gage test setup up.

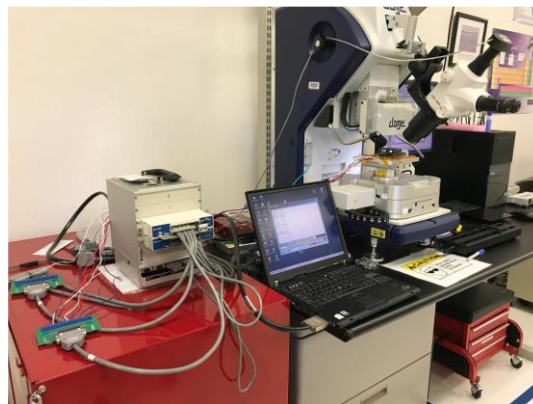


Figure 2. Button push and strain gage measurement setup

## Results

### *Microstructural Analysis on the Failed Samples*

From the dye and pry test on sample 1 from group 1, the solder joints in A14-17, B16,17, C17, E17 and G17 were identified with failures, where either full or partial red colored regions were observed. Figure 3 (a) shows one representative solder ball A17 in sample 1 at the PCB side after Dye and Pry testing. The presence of red dye indicates cracks in the area of interest. To further understand the failure mode of the solder joint, the BGA package in sample 2 from group 2 was cross sectioned in row A17-Q17 and column A1-A17, where failures were found from Dye and Pry tests. Figure 3(b) shows the cross section

image of a Sn-Cu solder joint A17 in sample 2. A brittle crack was observed all across the solder ball on the PCB board side. Non-destructive X-Ray analysis was also performed on the BGA of sample 2, which also clearly show cracks in the solder ball of A17 and B17, as shown in Figure 3(c). A similar fracture mode between the solder joint and the board pad was observed in row A17-Q17 and column A1-A17, which was identified as the cause of the product failure.

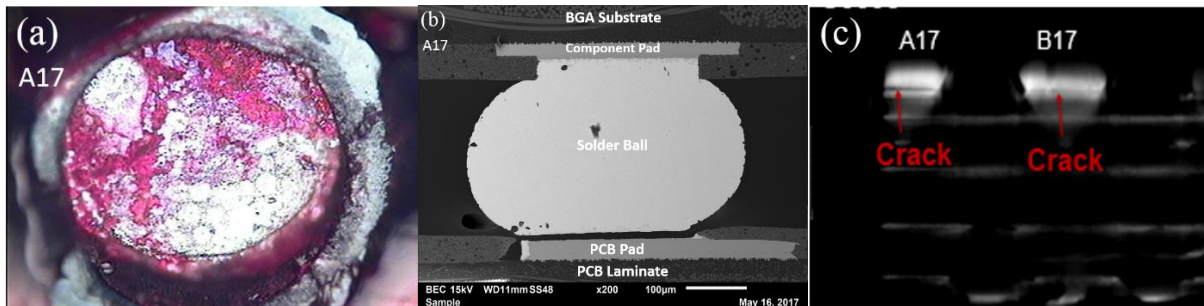


Figure 3. (a) Solder ball microscopy image after dye and pry on the PCB side; (b) SEM image of the cross-section area of a solder ball; (c) X-ray image of the cross section of the solder ball showing cracks.

Figure 4 (a) and (b) show the cross section image of solder ball C17 in sample 2, where a crack just initiated from the edge between the solder ball and the pad on the PCB side. By using a back scattered detecting mode, clear contrasts between different compositions were seen. Figure 4 (c) shows the image of the crack at a high magnification of 3300X. The crack was observed located between the Nickel-Tin (Ni-Sn) Intermetallic Compound (IMC) and the nickel layer of the Electroless Nickel Immersion Gold (ENIG) surface finish on the Copper (Cu) Pad. On top of the nickel surface, a thin dark grey nickel layer with identifiable spikes and corrosion cracks was observed. This is a symptom for the “Black Pad” defect that was usually observed in the PCB with the ENIG surface finish. Several mechanisms contribute to the “Black Pad” defects, i.e. creation of a thick Phosphorous enriched Ni<sub>3</sub>P layer at the electroless nickel (EN) surface, extensive corrosion of the exposed nickel surface and entrapment of EN plating residues beneath the gold coating. A combination of these mechanisms renders difficulty in wetting and the formation of a proper IMC layer during soldering. As a result, the solder joint becomes weaker when exposed to stress, and a fracture may occur between the IMC layer and nickel surface. This defect is called black pad since the nickel surface at which a crack occurs is usually dark grey to black due to the phosphorous enrichment. [ref.1-3]

To further confirm and understand the “Black Pad” defect, SEM imaging combined with EDX analysis was performed on sample 2 in solder joint C17. Comparisons of composition were made among the IMC area between the solder joint and the ENIG surface finish (spectrum 1), the “Black Pad” layer (spectrum 3) and the nickel layer on top of the copper (Cu) pad (spectrum 2), which is shown in Table 1. Figure 5 shows a SEM image of these three regions. In the intermetallic region Spectrum 1, gold was found in the Sn-Ni IMC layer. This indicates that during the soldering process, solder melts on the top layer of the ENIG surface finish, and the gold plating dissolves into the molten solder. In Spectrum 2 on the electroless nickel layer, a Phosphorus (P) content of 6.99 wt% was obtained, while in Spectrum 3, a higher P content of 10.09 wt% was found. This confirms an enrichment of P at the uppermost EN surface, which was caused by the extensive nickel dissolution into the molten solder. From the SEM image shown in Figure 4(c), several cracks were observed penetrating deeply into the Ni layer. This is an indication of extensive corrosion of the exposed nickel surfaces, where over-etching occurs with more Ni cations released into the immersion gold. Several studies have found that the main cause for the nickel corrosion is the not well-controlled EN plating that deposited nickel with an irregular topography [ref.1-4]. In the EN coating, an irregular topography with distinct crevices has a great tendency for corrosion compared to an even topography. Irregular topography can be caused by a nickel bath running outside its control limits, contaminated copper pad surface or inadequate pre-treatment. In Spectrum 2 and 3, tin (Sn) was found in the EN layer, and this is thought due to the deep penetration of molten solder following the gold plating into the nickel corroded area.

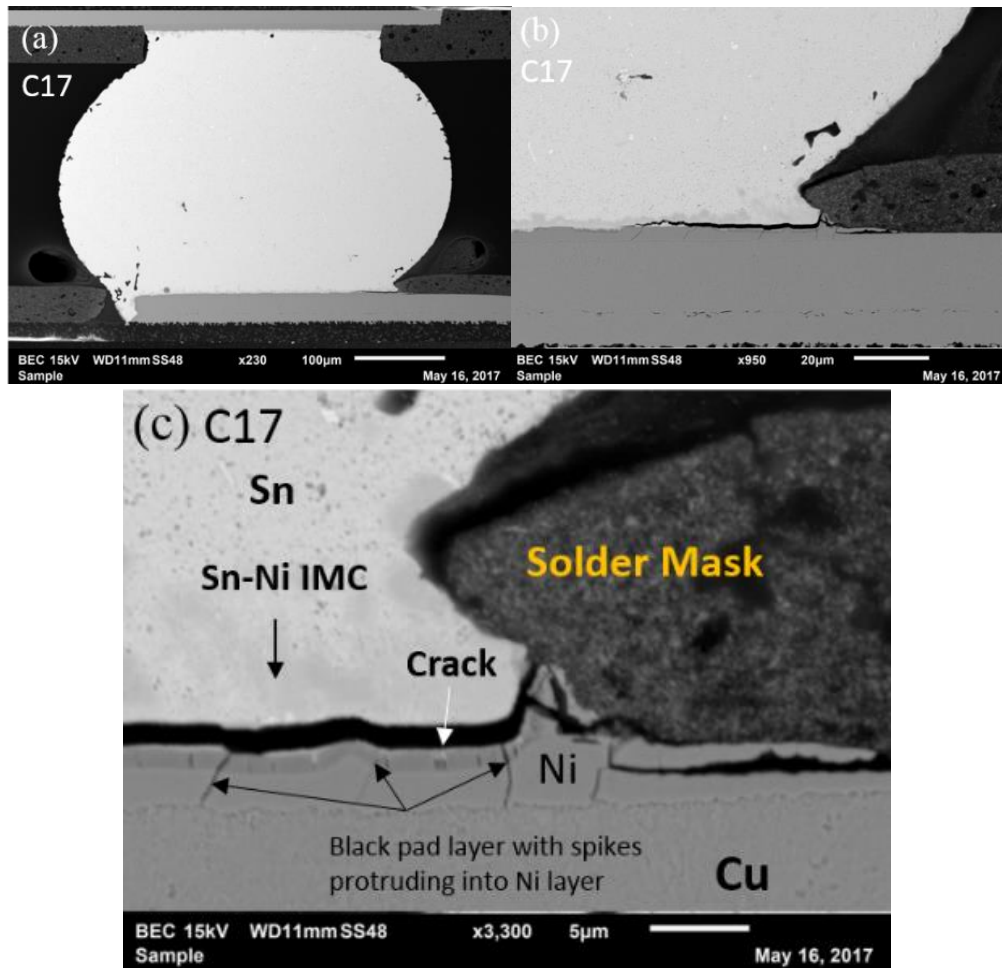


Figure 4. SEM image (back scattered mode) of solder C17 in sample 2 at magnification of (a) 230X; (b) 950X; (c) 3300X. The IMC, Ni layer and the black pad area are marked.

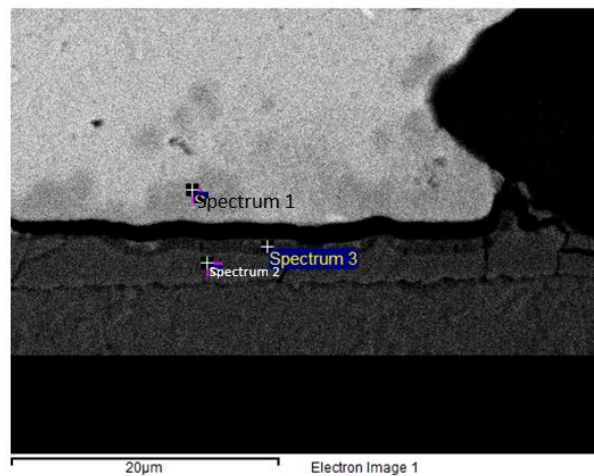


Figure 5 SEM Image of Sample 2 Solder C17 showing different regions for EDX analysis

Table 1. Comparisons of compositions in the IMC layer (spectrum 1), black pad layer (spectrum 3), and the Nickel layer (Spectrum 2)

	Ni (wt%)	Cu (wt%)	Sn (wt%)	Au (wt%)	P (wt%)
Spectrum 1	9.15	16.8	51.04	3.15	0
Spectrum 2	53.7	5.41	7.01	0	6.99
Spectrum 3	37.01	4.8	15.94	0	10.09

In summary, the “Black Pad” failure was mainly caused by the not well-controlled ENIG process and the brittle phosphorous-enriched Ni-P thin layer. Several approaches are proposed to minimize or eliminate this failure. One approach is to improve the whole ENIG process, including careful pre-treatment before nickel gold deposition, and well-controlled processes in the EN plating and the immersion gold plating. In the pre-treatment process, it is vital to ensure a clean surface after micro-etching of the copper, and the PCB needs to be properly dried to prevent localized corrosion of the copper pad. In the process of EN plating, slower deposition rates are preferred to minimize deep crevice formation at grain boundaries, so that corrosion during immersion gold plating can be reduced. It is also important to control the reaction temperature and pH to achieve a uniform surface morphology with minimum crevices at grain boundaries. In addition, the aggressiveness of the gold bath can be prevented by controlling gold plating thickness within 0.05-0.10  $\mu\text{m}$  per the IPC-4552 specification. The plating rate should also be controlled to not be too fast. [ref.1-4]

Since “Black Pad” failure is usually associate with ENIG surface finish, several alternative plating methods can be used to eliminate the “Black Pad” failure. For example, Electroless Nickel Electroless Palladium Immersion Gold (ENEPIG) showed substantial advantages to meet multiple requirements of miniaturization, thinness, solder joint reliability, gold wire bondability, and excellent shelf life. It plates a layer of electroless palladium onto the nickel prior to immersion gold plating, which eliminates the potential for excessive gold plating solution attack on the EN surface. However, ENEPIG is costly, which involves a more complicated plating process. Other alternative surface finishes could also be considered, such as OSP (Organic Solderability Preservative), or IAg (Immersion Silver). Both surface finishes have advantages and disadvantages, so careful decisions need to be made considering the applications. For example, with OSP, the thickness cannot be measured, because it is clear and transparent. It also has short shelf life, and it exposes copper on final assembly. Also Immersion Ag is more susceptible to corrosion attack at elevated temperatures and humidity environments. [ref.4]

**Low Strain-Rate Cyclic Button Push Tests**

From the failure analysis of the field returned samples in group 1, brittle fracture mode was observed because of the “Black Pad” failure. Besides consideration of high strain-rate events such as drop, high strain induced deformation could also increase the reliability risk of the portable consumer product. When evaluating the product design, the failed BGA package was found to experience cyclic high strains at low strain rate during operation. Thus, it is necessary to investigate the failure mechanisms of the BGA under this cyclic low strain-rate loading at a high strain level. Before performing the low strain-rate cyclic push tests, a few single cycle button push tests were conducted to understand the strain level at three different conditions, i.e. at the minimum force activating the button (where the button was on the external enclosure), at the minimum force activating the switch (remove external enclosure), and in a regular human operation condition. A constant loading speed was applied at 0.1 mm/s.

Figure 6 shows that four strain gages were installed around the BGA on the PCB board. Strain gages were chosen to be installed to places where no components were in place. In addition, from the board design, the switch was located near the top left corner of the BGA as illustrated in Figure 6, so strain gage 1, 3 and 4 were installed in that corner. Figure 7 illustrates the electronic device structure with the old button and new button on the enclosure, switch on the top side of PCB board, and the BGA on the bottom side of the PCB board. The switch is located near one corner of the BGA. The old button was made of rubber material, while new button was made of plastic material, which is softer than the rubber material.

Figure 8 shows the strain variation with the one cycle button push. When there is a load drop and a strain drop, the maximum force before the drop was recorded as the minimum force to activate the button. For human operating tests, a few button push tests were performed by two persons, and the maximum strain was recorded. Figure 9 shows the strain variation upon a few cycles of human button push tests for both the old design and new design. Figure 10 compares the strain at the minimum force activating the button, switch and in real operation conditions. For all three conditions, the new design shows a much lower strain level than the old design, which indicates an improvement in structural design to lower the impact of board bending. Because the plastic materials in the new button are less rigid than the rubber materials in the old button, the stress applied to the new button can be much lower, thus the strain levels are usually lower in the new button push tests. The strain at the minimum force activating the button and switch fall within the IPC/JEDEC-9704 standard [ref. 5] for both the old

design and new design. However, the strain level of 700  $\mu\epsilon$  in the old design and 500  $\mu\epsilon$  in the new design for human operation conditions are approaching the limit of IPC/JEDEC-9704 standard, which could be a potential risk for failures.

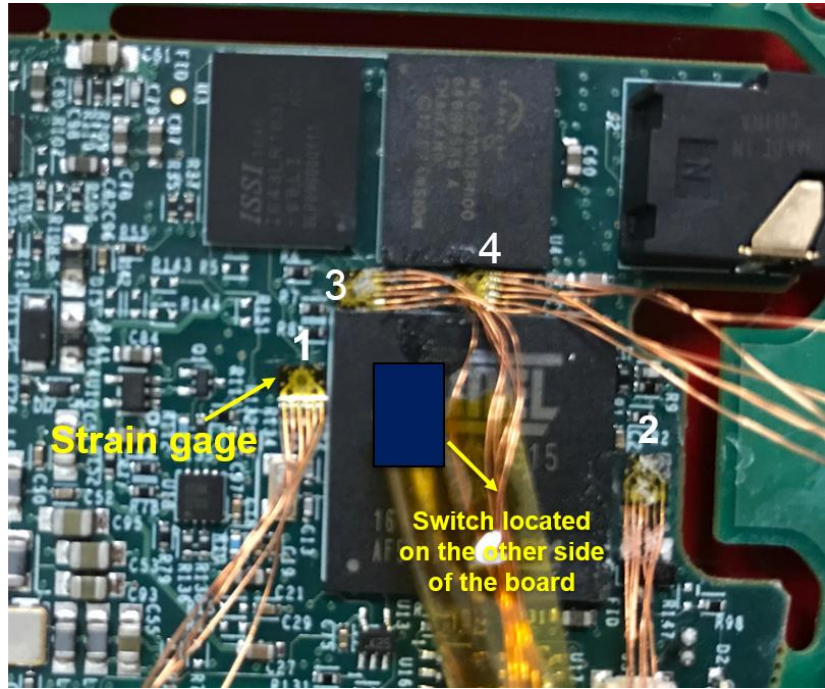


Figure 6. Four strain gages installed around the BGA

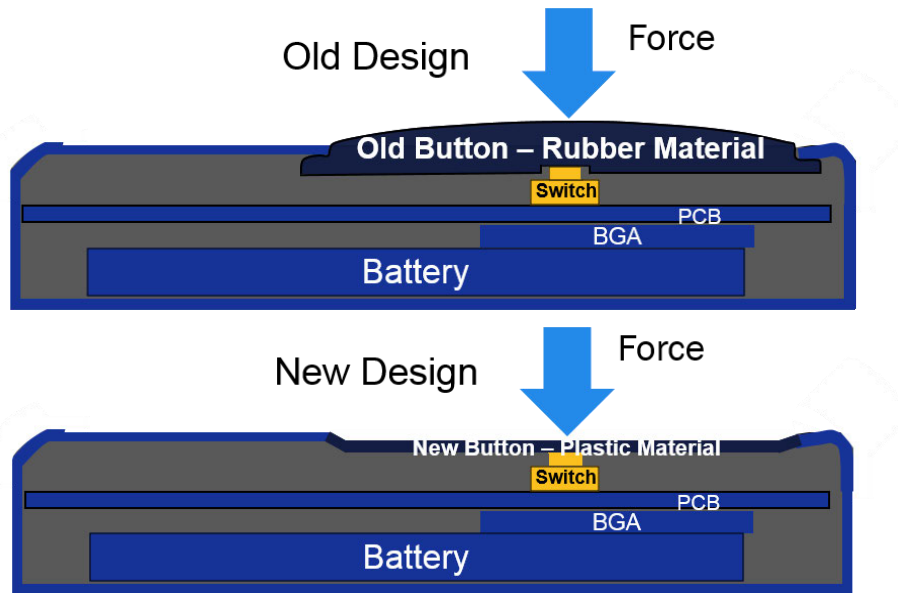


Figure 7. Schematic of cross sectional view of the old button and new button push test on the electronic device

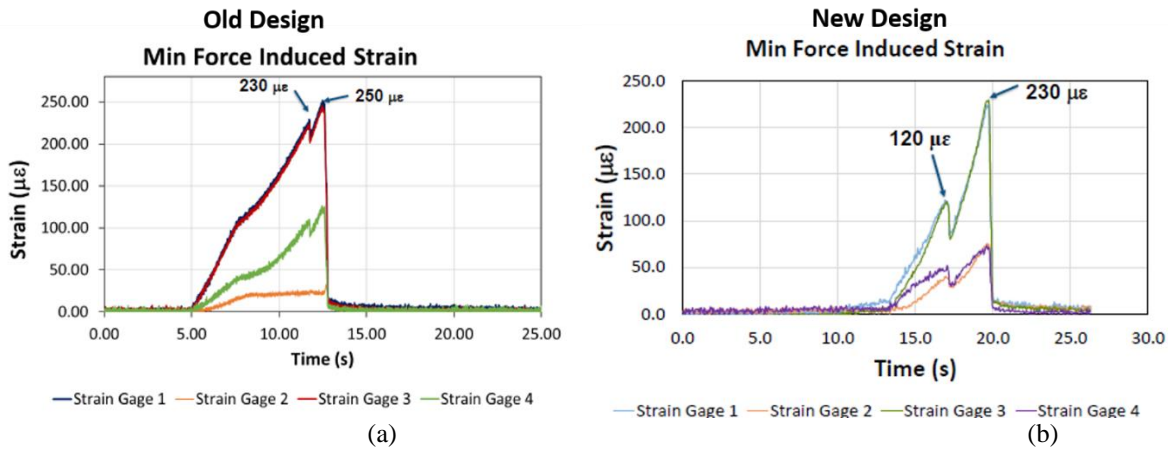


Figure 8. Strain changes upon one cycle of button push test with minimum force to activate the button for (a) old design, and (b) new design

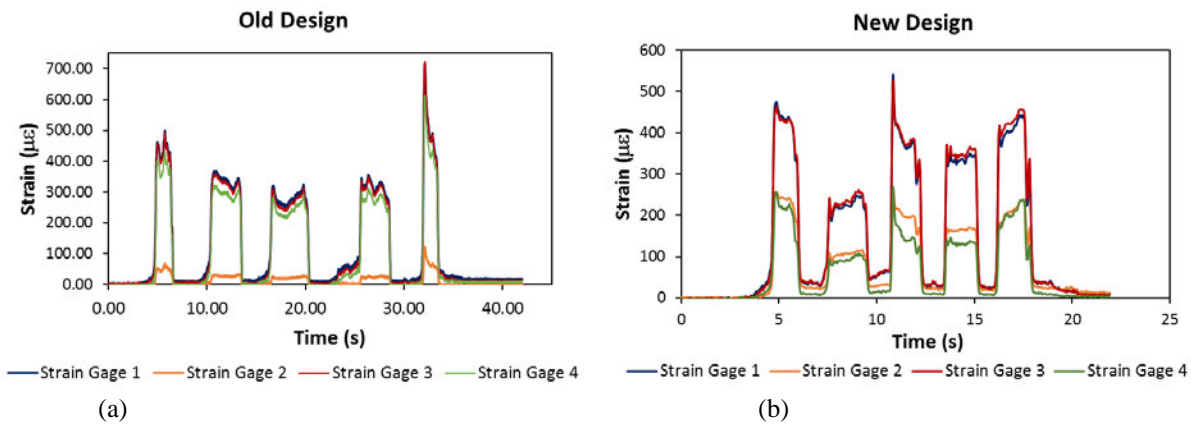


Figure 9. Strain changes upon human button push tests for (a) old design, and (b) new design

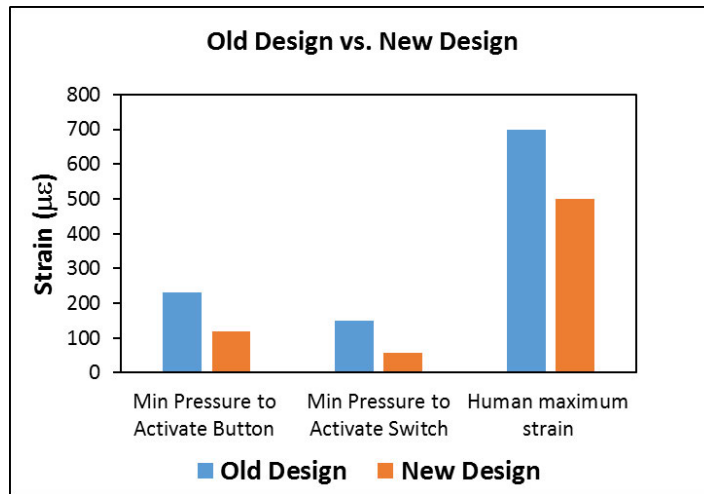


Figure 10. Strain at minimum force to activate the button, switch and in real operation conditions

To further understand how the high strain in human operating conditions affect the performance of the product and the failure mechanisms, low strain-rate cyclic button push tests were performed at the product level for both the old design and new design. The testing speed is 13 seconds/cycle, including 10 seconds of push holding time. This testing condition is very close to a real operating condition. The tests were stopped at 40,000 cycles, which is equivalent to about 3 months' usage time. Functional tests were done for every 8000 cycles, and both products were still functional after 40,000 cycles.

Figure 11 (a) and (b) shows the strain changes during the low strain-rate cyclic button push tests for the old design and new design. Four strain gages were installed around the four corners of the BGA, which were labeled as strain gage 1,2,3,4. The strain gages that show the highest level of strain were used for comparison studies. The strain differences in the different strain gage indicate that the BGA experienced non-uniform strain and stresses. Figure 12 (a) and (b) show the cracks in the solder joints in the old design product, and Figure 13 (a)-(d) show the cracks in the solder joints in the new design product. Three failure modes were identified. The first failure mode was the same as seen from Figure 3 (b), i.e. a brittle crack between the solder joint and the copper pad, which is because of the “Black Pad” effect. The corroded Ni layer made it weak at the interface between the IMC layer and the pad, thus cracks are prone to initiate in this area. The second failure mode is the ductile fracture in the bulk solder part that is close to the pad on both board side and component side. The third failure mode is the crack in the IMC at the board side. Figure 12 (a), (b) and Figure 13 (a) show a mixture of the failure modes mentioned above. The brittle cracks were thought to be first formed at early stages of the cyclic button push tests, and the ductile cracks were later formed at longer cycles of button push tests. Similar failure modes were also observed in Sn/Pb Solder joints from thermal cycling tests. [ref.6] Figure 13 (b), (c) and (d) show the ductile crack mode that initiated after long cycles of bending from the button push. Cracks tend to initiate at the edge of the pad that connect to trace lines, which are thought to be due to the high stress concentrations in these regions.

The differences of the three failure modes were attributed to several factors, i.e. strain rate, loading angle, and the IMC layer roughness. A ductile-to-brittle transition was observed with increasing strain rate [2, 3]. At low strain rates, the fracture mainly occurs through the solder, while at high strain rates, the crack path transferred into the IMC layer or at the interface between the IMC and the solder. The brittle cracks observed from the two failed samples are thus more possibly formed during a high strain rate event, such as during drop or vibration. In addition, in the button push tests, the solder joints were subjected to compressive stresses. In real applications, mix-mode loading conditions, e.g. mixed compressive and shear forces were usually applied to the solder joints. A few studies found that an increase in the loading mode-mixity (loading in multiple directions) could enhance the proclivity of a solder joint towards brittle failure. [ref.7] This might also explain why more brittle cracks were found in the failed samples. Furthermore, the IMC roughness was found to affect the fracture mode of the solder joint. The crack is more prone to propagate through the ductile solder with smooth IMC, while a brittle crack is more likely to form in a rough IMC layer. From Figure 12 and Figure 13, the cracks were mostly located inside the bulk solder, which indicate relative smooth IMC was formed.

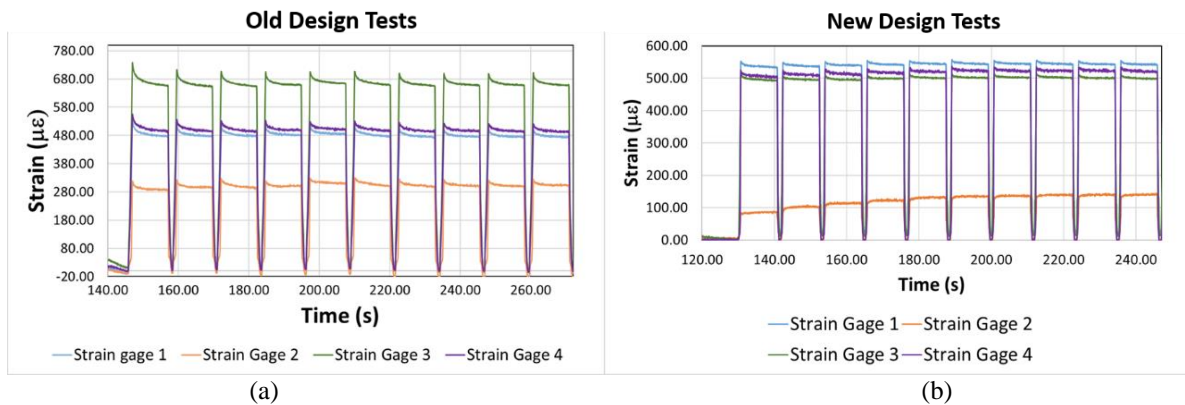


Figure 11. Strain changes during the low strain-rate cyclic button push tests for (a) old design, and (b) new design

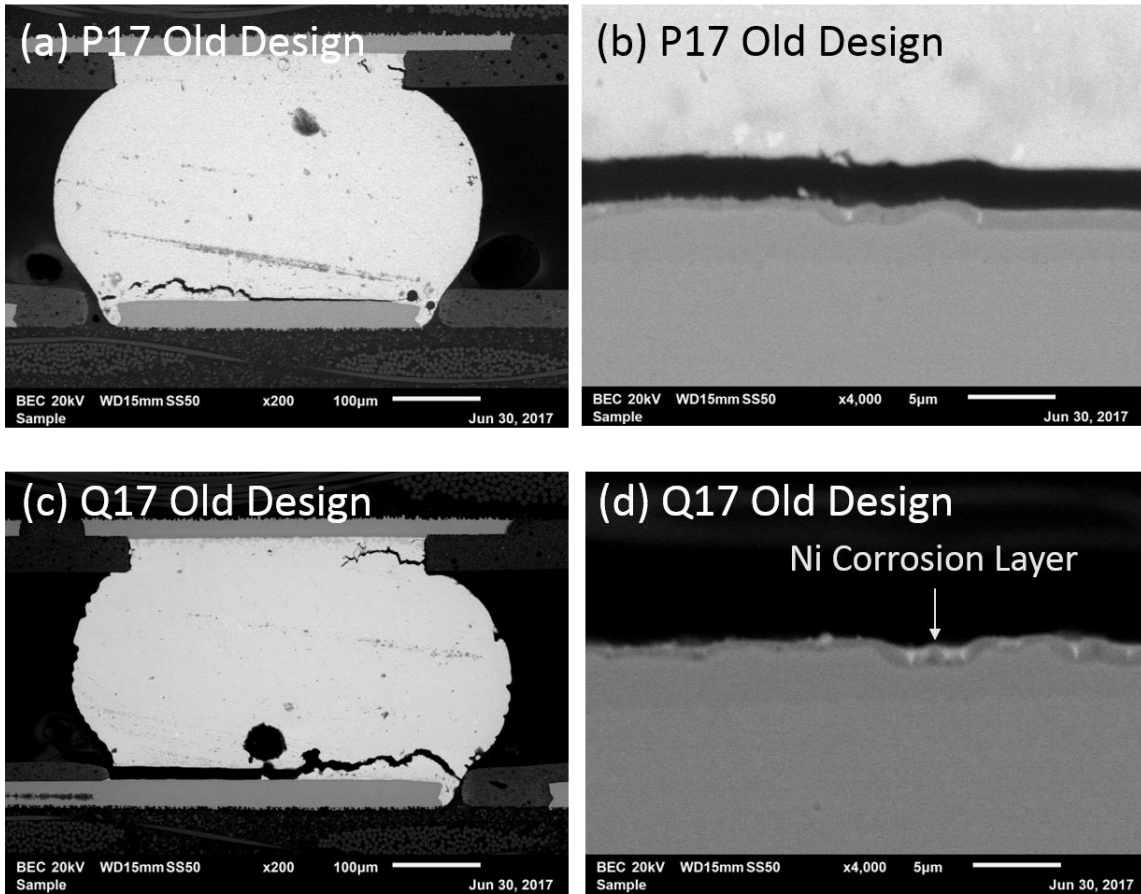


Figure 12. SEM images of the solder ball (a) P17 and (b) Q17 in the old design product after 40,000 cycles of low strain-rate cyclic button push tests.

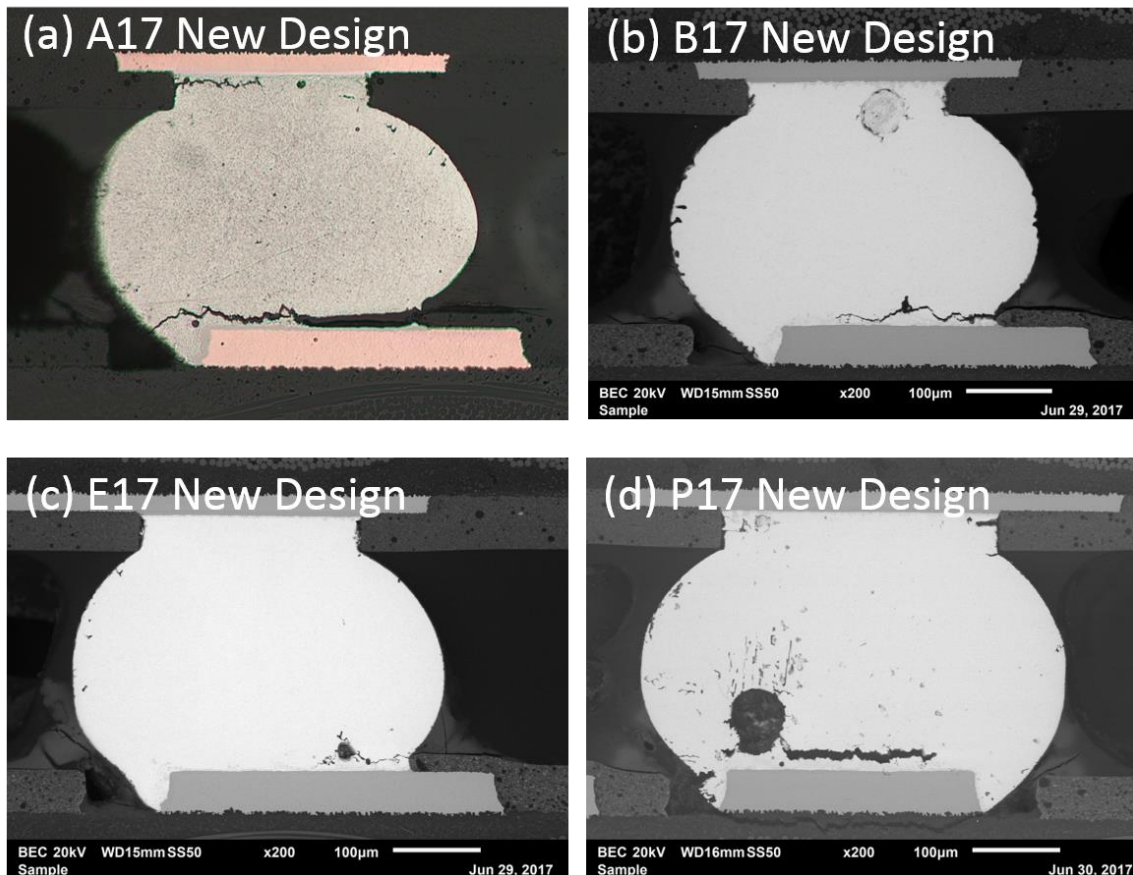


Figure 13. SEM images of the solder ball (a) A17, (b) B17, (c) E17 and (d) P17 in the new design product after 40,000 cycles of low strain-rate cyclic button push tests.

## Conclusions

In this study, failure mechanisms of Sn-Cu solder joints in a BGA assembly were investigated. “Black Pad” failure was found in the failed samples, which was mainly caused by the not well-controlled ENIG process and the brittle phosphorous-enriched Ni-P thin layer.

In addition, failure mechanisms of the solder joints under cyclic low strain-rate loading were also investigated. From the strain gage measurement, it was found that by improving the enclosure design structure and materials, the strain level can be reduced. A mixture of brittle cracks from “Black Pad” failure and ductile cracks in the solder or in the IMC were observed. The differences of the three failure modes were attributed to several factors, i.e. strain rate, loading angle, and the IMC layer roughness. Furthermore, brittle cracks are more prone to be formed when subjecting to loading from multiple directions with a rougher IMC layer.

## ACKNOWLEDGMENTS

The authors would like to thank all Advanced Engineering Group (AEG) members from Flex International for valuable discussions and suggestions.

## References

1. P. Tegehall, “Review of the Impact of Intermetallic Layers on the Brittleness of Tin-Lead and Lead-Free Solder Joints”, IVF Project Report 06/07, 2007.
2. K. H. Lee, "Identification and prevention of “Black Pad” in Sn/Pb soldering", Circuit World, Vol. 37 Issue: 3, pp.10-15, 2011.

3. K. Zeng, R. Stierman, D. Abbott, et al., "The root cause of black pad failure of solder joints with electroless Ni/Immersion gold plating", JOM 58: 75, 2006.
4. J. Nable, "PCB Surface Finishes: A General Review", SMTnet, June, 2015.
5. IPC/JEDEC-9704, "Printed Wiring Board Strain Gage Test Guideline", 2005
6. M. Meilunas, A. Primavera, and S. O. Dunford, "Reliability and failure analysis of lead-free solder joints", IPC Conference, New Orleans, LA, November 2-3, 2002.
7. P. Kumar, Z. Huang, I. Dutta, "Roles of process and microstructural parameters of mixed mode fracture of Sn-Ag-Cu solder joints under dynamic loading conditions", Proceedings of InterPACK, Paper no. 89205, IEEE/ASME CD-ROM, 2009.

# **Solder Joints Failure Under Low Strain-rate Cyclic Loading**

Jie Lian, Ph.D., Dennis Willie, Jada Chan, Francoise Sarrazin, Ellen Ray, Kelvin Wong, Christopher Vu,  
Wesley Tran, Tuyen Nguyen, Tu Tran, Anwar Mohammed, Ph.D., Michael Doiron

FLEX International

Milpitas, CA

# Outline

- Objective
- Part I – Field Returned Units
  - *Failure Analysis using Dye & Pry, Cross Section, X-Ray, and EDX analysis*
  - *Failure Mode Analysis*
  - *Conclusions*
- Part II – Experiments of New Units to Simulate Failures
  - *Cyclic Button Push Tests on Brand New Functional Units*
  - *Failure Mode Analysis*
  - *Conclusions*
- Design Improvement and Results
  - *Reduced strain from button push through change of button material and button structure*
- Conclusions
- References & Acknowledgement

# Objective

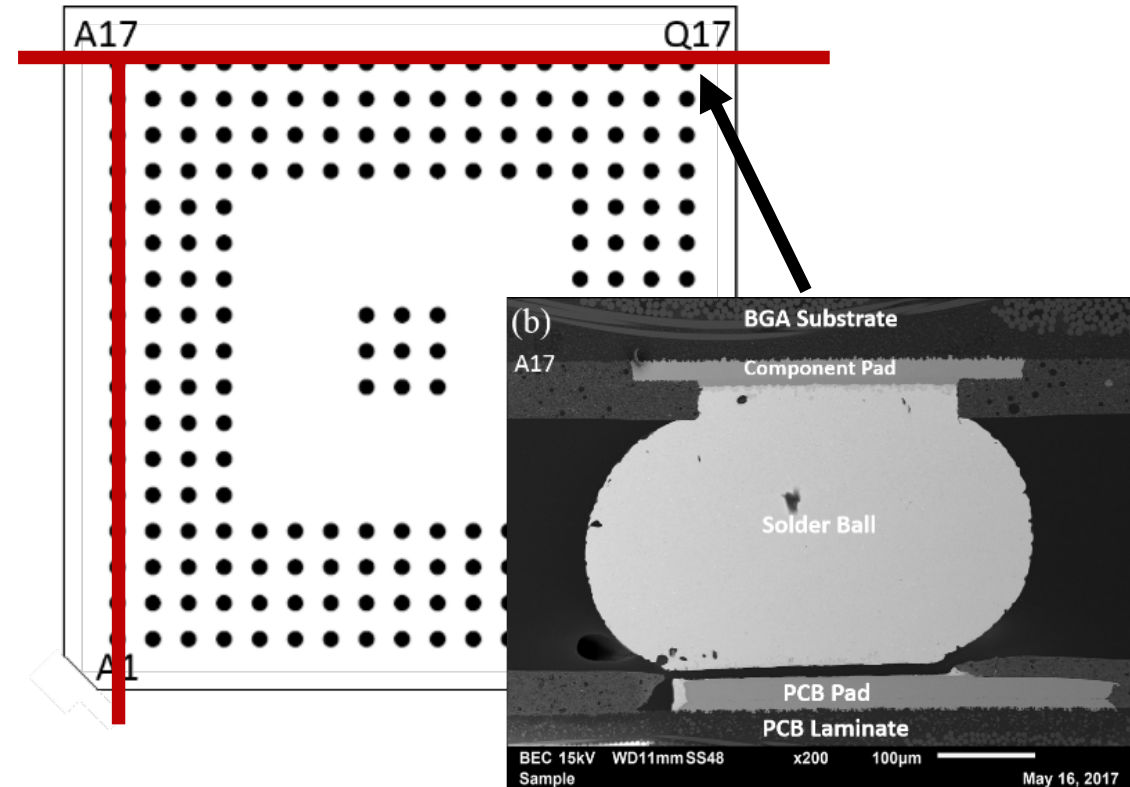
## FA Case Study

- Identify the root cause of failure in a consumer portable product
- Utilize various failure analysis methods to assess the failure mode
- Learn about how different factors (such as loading conditions, selection of surface finish and package structure) affect the failure mode of SAC305 (Sn-Ag-Cu) solder joints
- Seek improvement of structural design reliability
  - *Validate Push Button material & structural changes that improve reliability*
- Understand the failure mode under cyclic mechanical bending at the product level

# Part I – Failure Analysis of BGA Assembly in Field Returned Units

## Failed product background

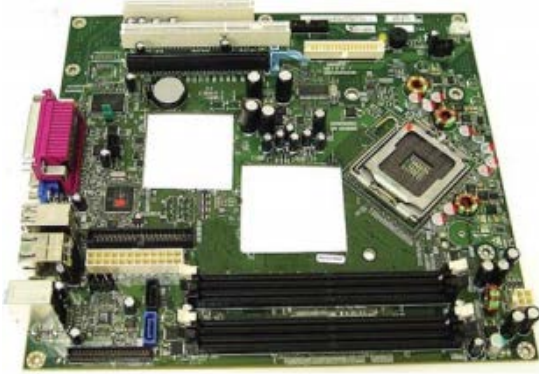
- High failure rate was found in a consumer portable electronic device
- Based on electrical function tests, the BGA was found to be the main failed part
- Failing BGA Device subjected to repeated bending stresses during operating conditions
- Failure analysis plans including dye & pry, cross section and X-ray analysis were proposed to identify the failure locations and learn about failure mode



*BGA land pattern with solder ball numbers labeled with picture of Solder Ball separated from PCB Pad.*

# Part I – Dye & Pry Tests

## IPC-TM-650 Standard for Dye & Pry of SMT Components



Cut Component from the Board



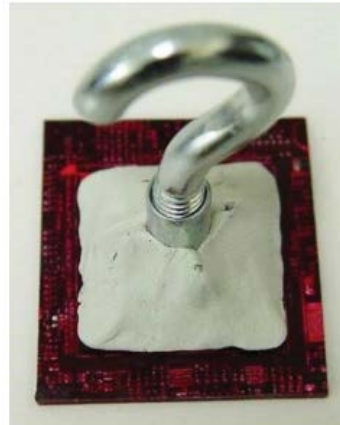
Clean Sample in Liquid Flux-Removing Solvent



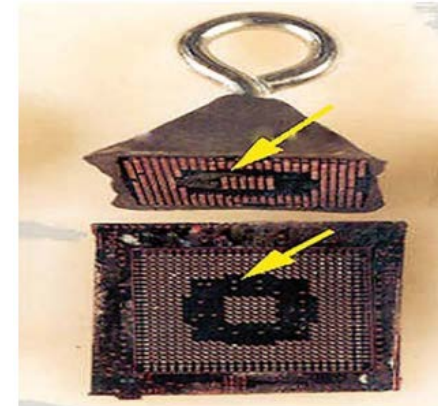
Clean Sample with Spray Flux Remover



Sample Submerged in Dye



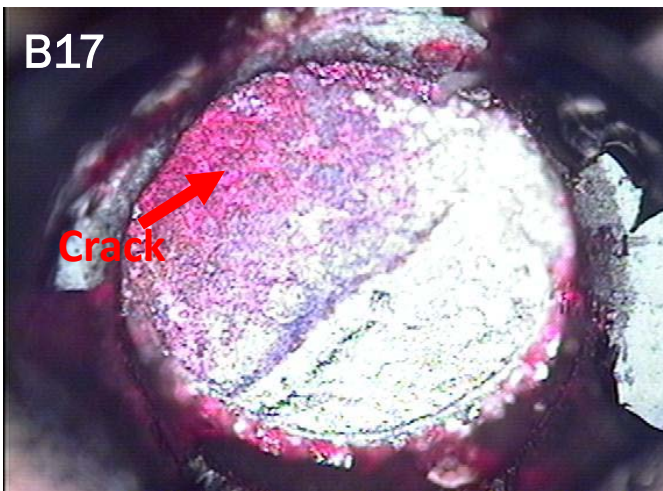
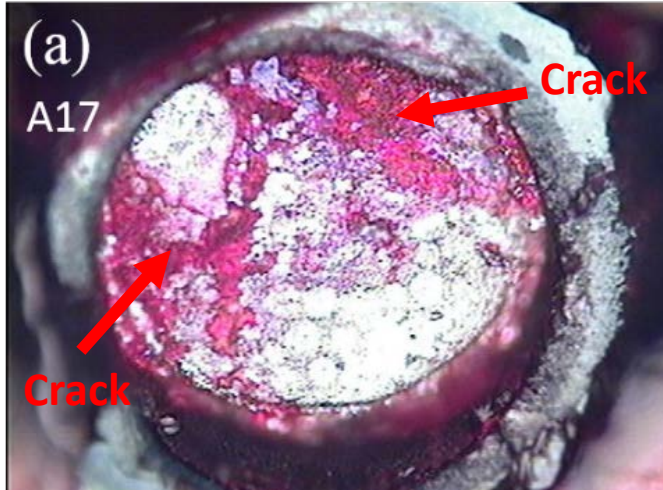
Sample Prepped with Tee Nut, Pull Hook and Molding Compound



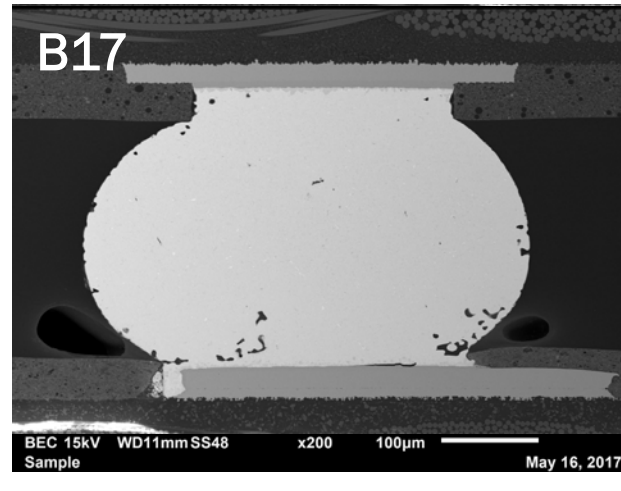
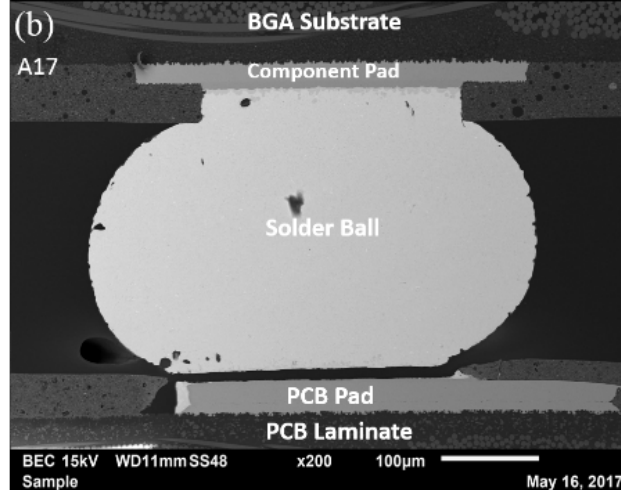
After Pull, BGA/SMT Part (top) and the Printed board (bottom)

# Part I Results – Dye & Pry, Cross Section and X-Ray Images

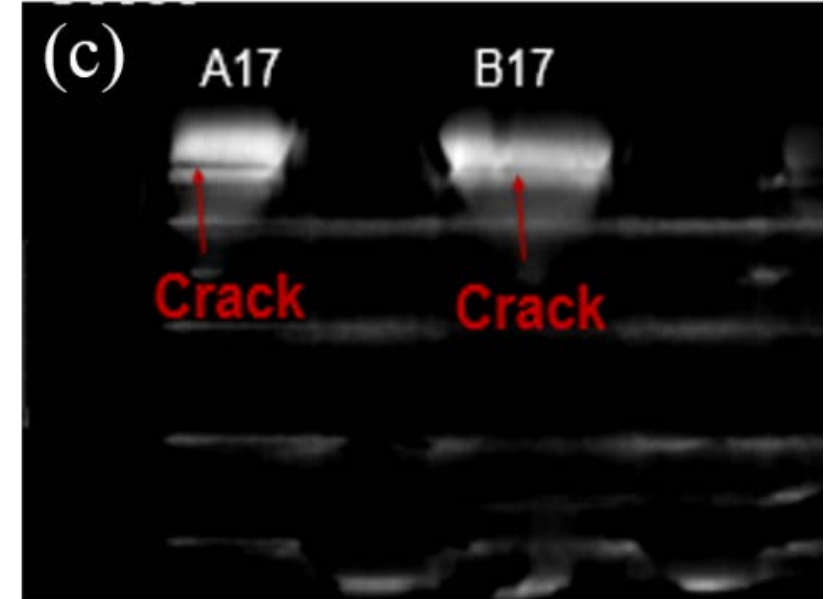
Solder Joint After Dye & Pry



Cross Section Images

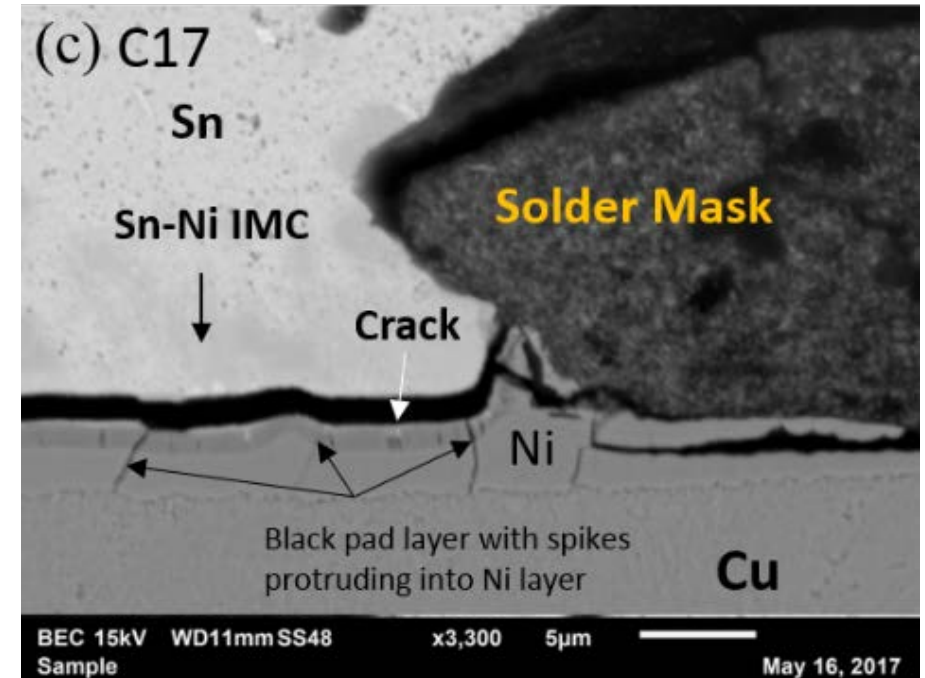
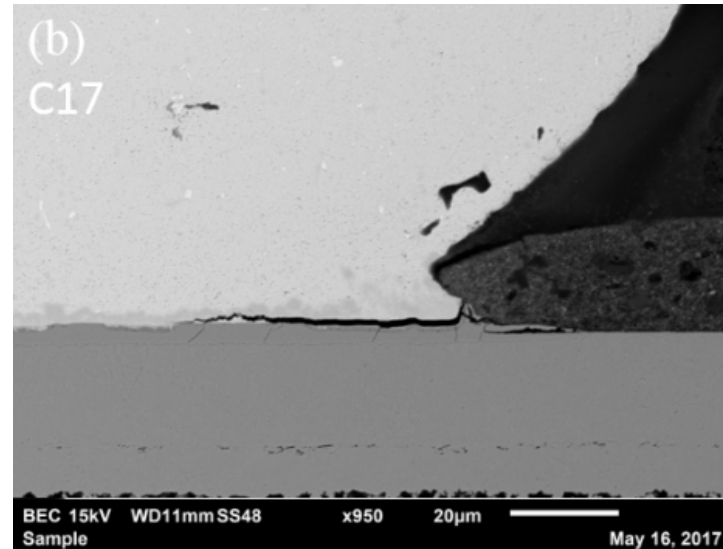
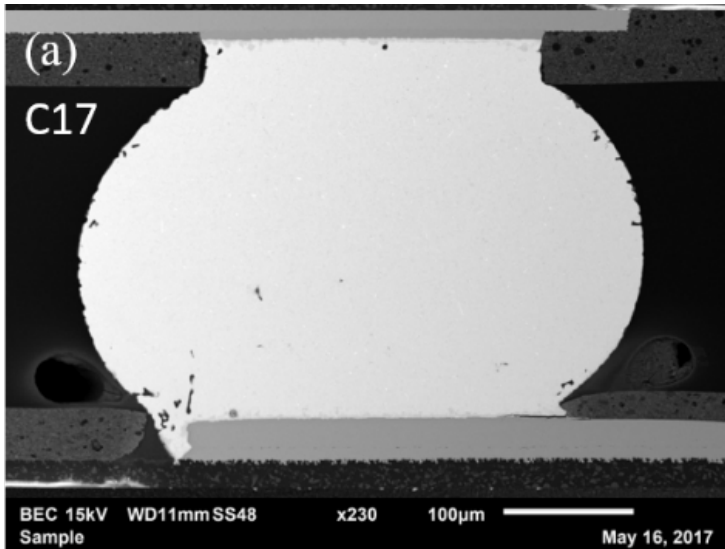


X-Ray Image



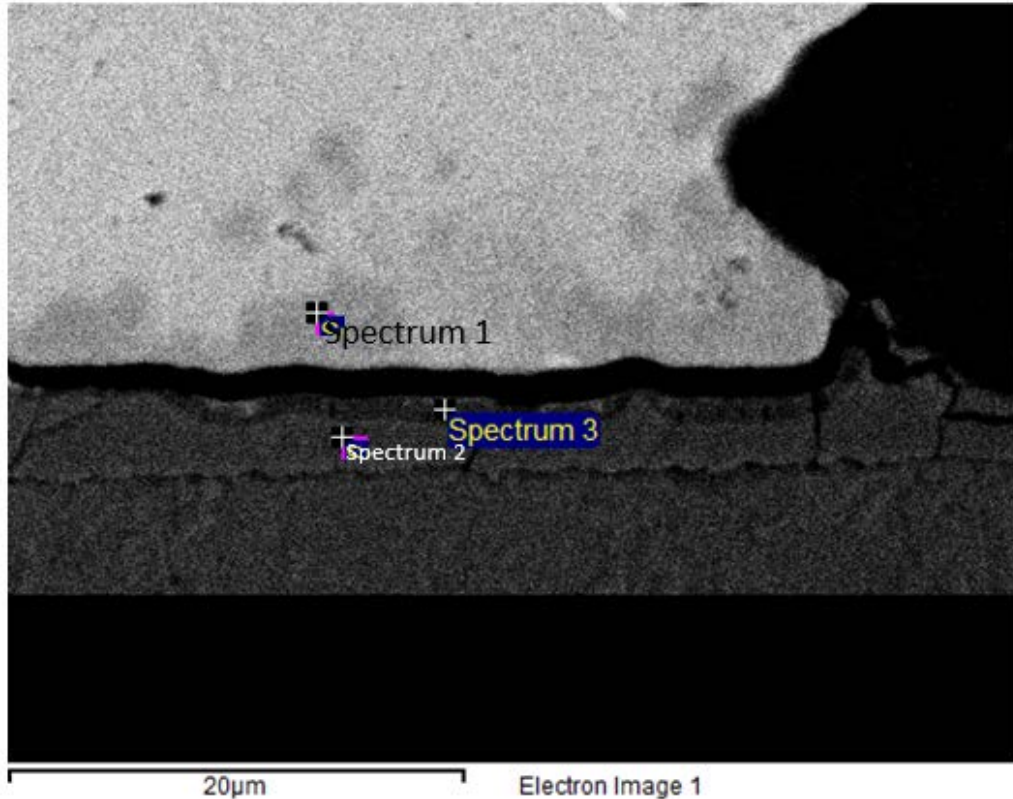
- Partial fractures were observed from Dye and Pry Tests in Sample 1
- Full and partial brittle cracks were observed from cross section and X-Ray Images

## Part I Results – Cross Section Images



- The brittle crack was observed located between the IMC and the ENIG surface finish
- “Black Pad” failure was identified from the thin dark grey Ni layer with identifiable spikes observed

# Part I Results – EDX Analysis



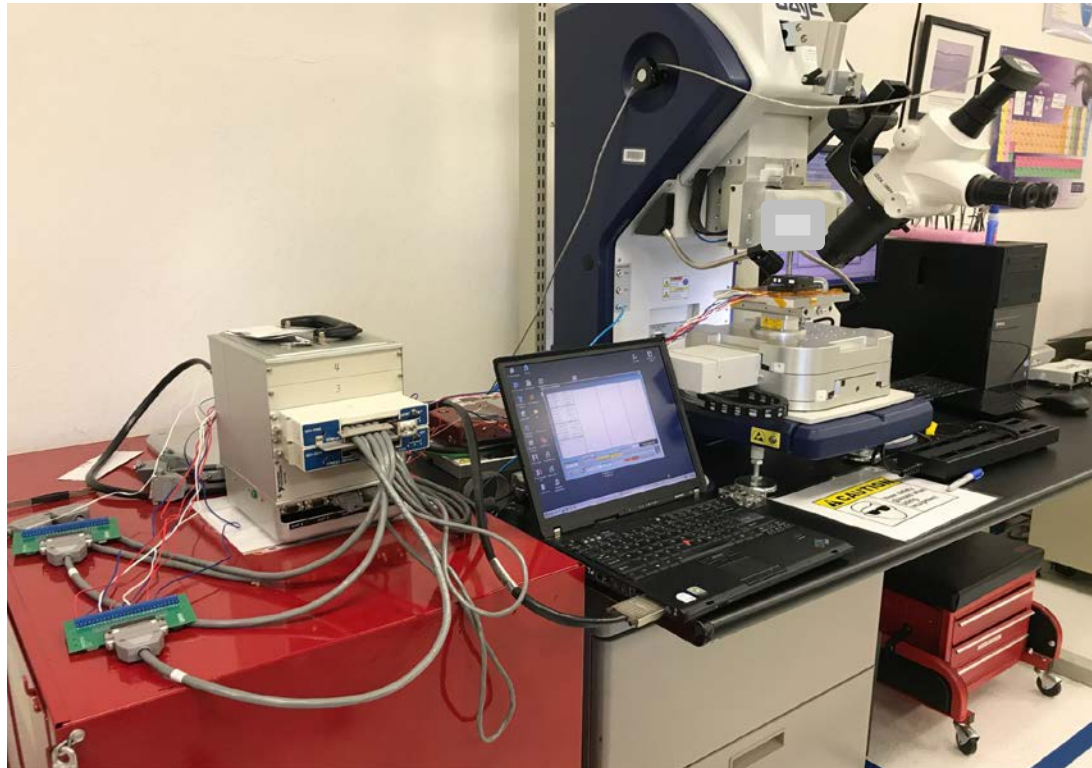
	Ni (wt%)	Cu (wt%)	Sn (wt%)	Au (wt%)	P (wt%)
Spectrum 1	9.15	16.8	51.04	3.15	0
Spectrum 2	53.7	5.41	7.01	0	6.99
Spectrum 3	37.01	4.8	15.94	0	10.09

- **Spectrum 1 (IMC layer):** No P in the Ni-Sn intermetallic layer
- **Spectrum 2 (Electroless Ni plating layer):** P content of 6.99 wt%
- **Spectrum 3 (“Black Pad” layer):** higher P content of 10.09 wt%

## Part I Summary – Black Pad Failure

- Failure Mechanisms: Solder joint is weak when exposed to high strain rate event
  - Extensive nickel dissolution into the SAC solder, which cause an enrichment of P at the uppermost of EN surface, and this layer is usually brittle and weak
  - Extensive corrosion of exposed nickel surface and entrapment of EN plating residues beneath the gold coating
- Improvement Methods:
  - Careful pre-treatment before nickel gold deposition
  - Well-controlled processes in the electroless nickel plating and the immersion gold plating
    - a. Slower deposition rates are preferred to minimize deep crevice formation at grain boundaries, so that corrosion during immersion gold plating can be reduced
    - b. Control the reaction temperature and pH to achieve a uniform surface morphology with minimum crevice at grain boundaries
    - c. Aggressiveness of the gold bath can be prevented by controlling gold plating thickness within 0.05-0.10  $\mu\text{m}$  per IPC-4552 standard. The plating rate should also be controlled not to be too fast.

## Part II – Mechanical Button Push and Strain Gage Test Setup

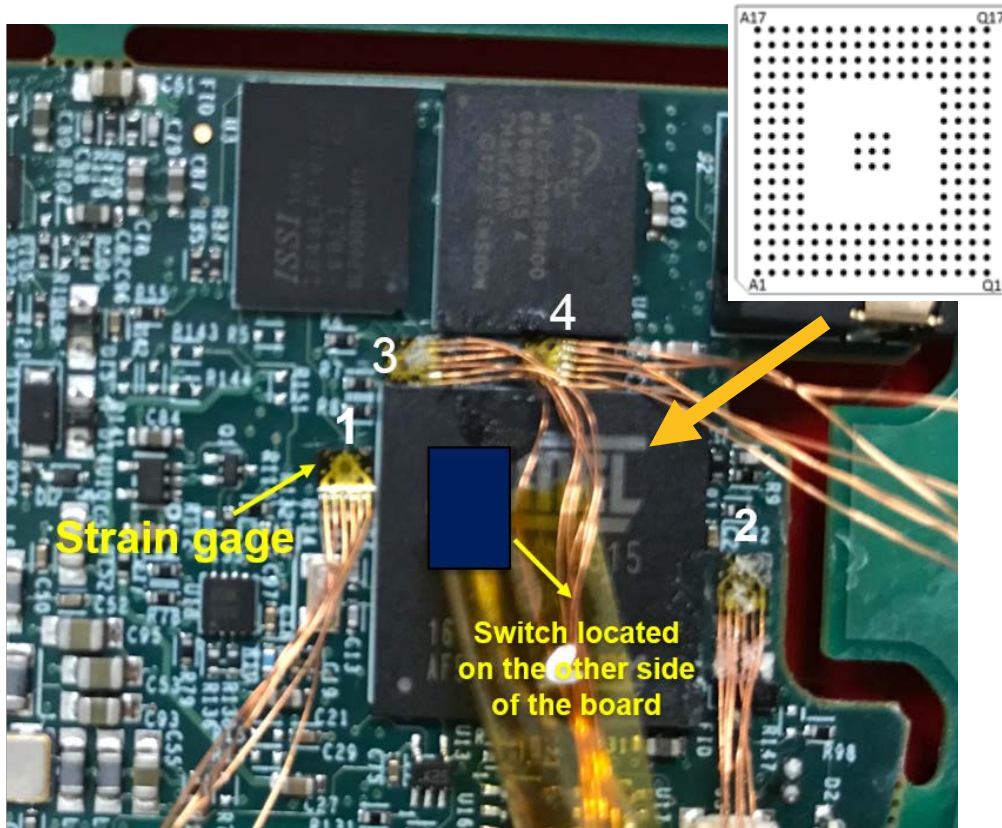


- Production Bondtester
- Strain Gage Measurement Setup: Strain Gage Measurement Setup: Production Chassis, with two strain modules

Button push and strain gage measurement setup

# Part II – Button Push Test Illustration

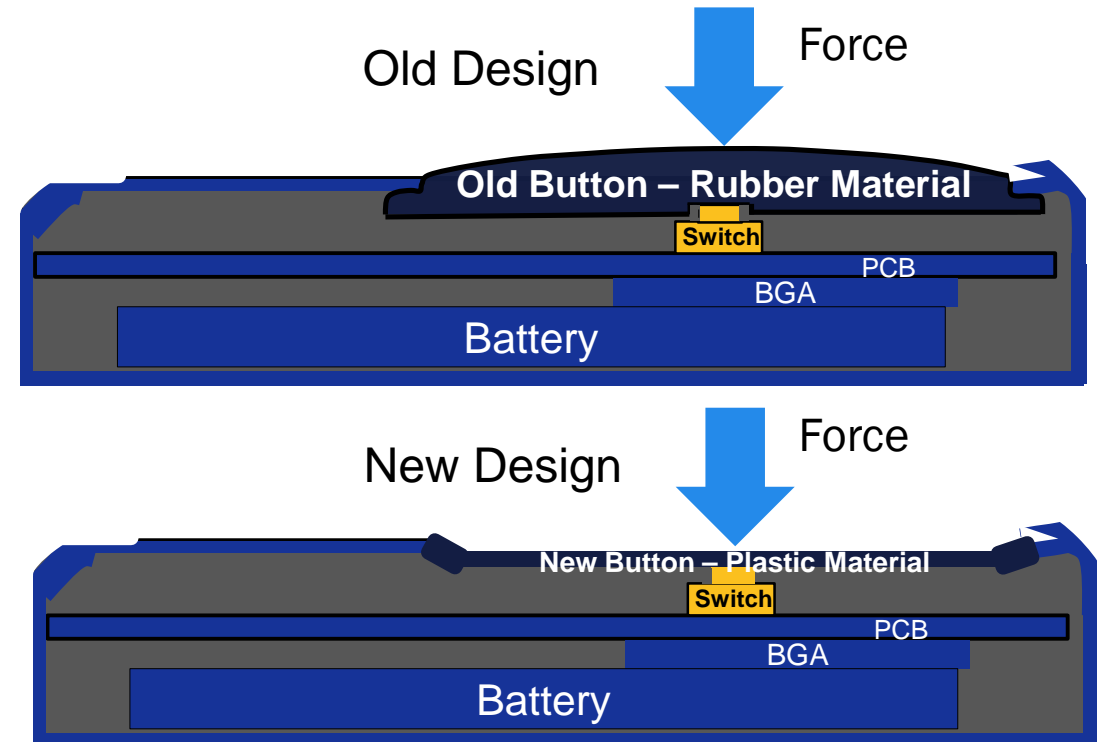
## Strain Gages Location



Switch is located close to the top left corner of BGA

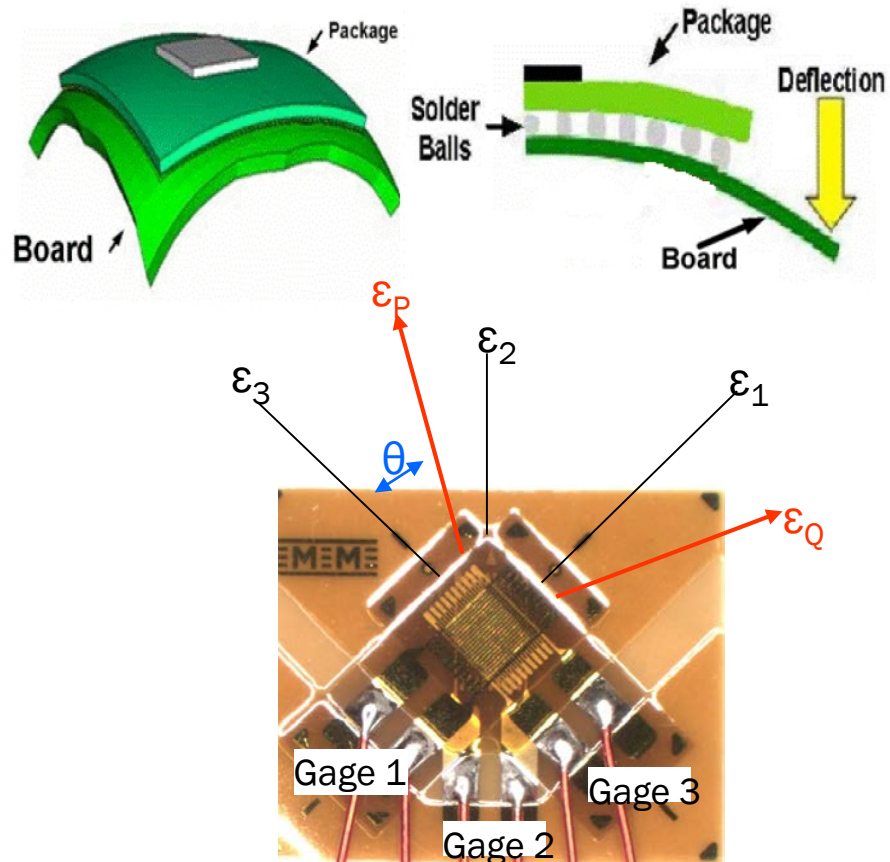
## Button Push Test

- Old Design: rubber materials; New Design: plastic materials
- Rubber is stiffer than plastic material, to gain same level of strain, the rubber button applied higher load



## Part II – Strain Gage Measurement

- To evaluate the PCB flexure during manufacturing and test operation processes

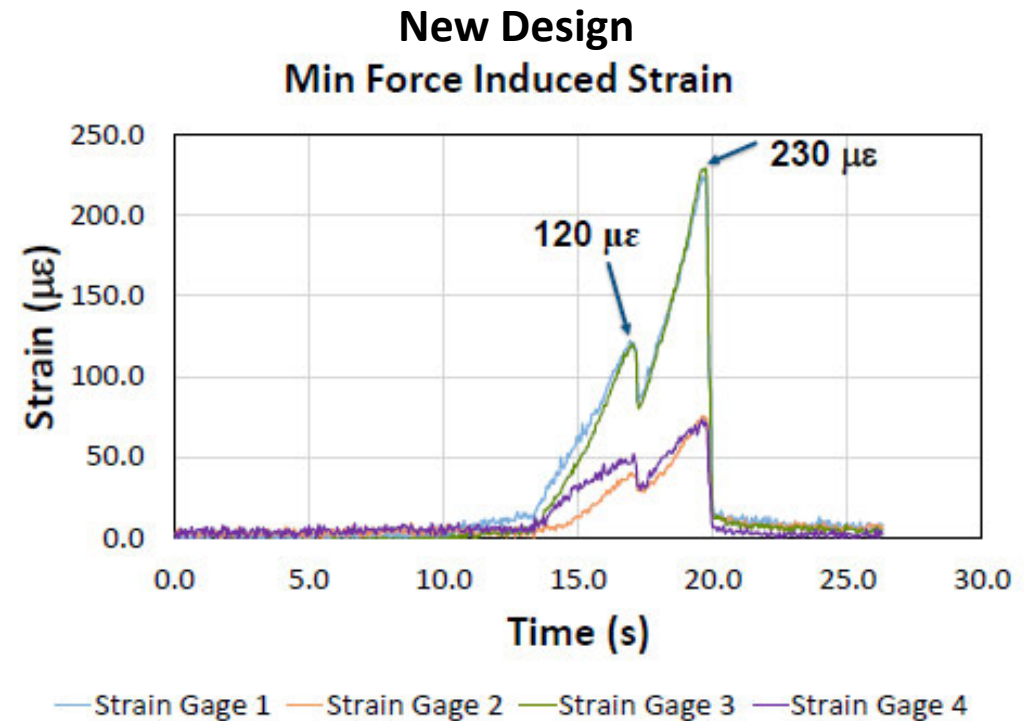
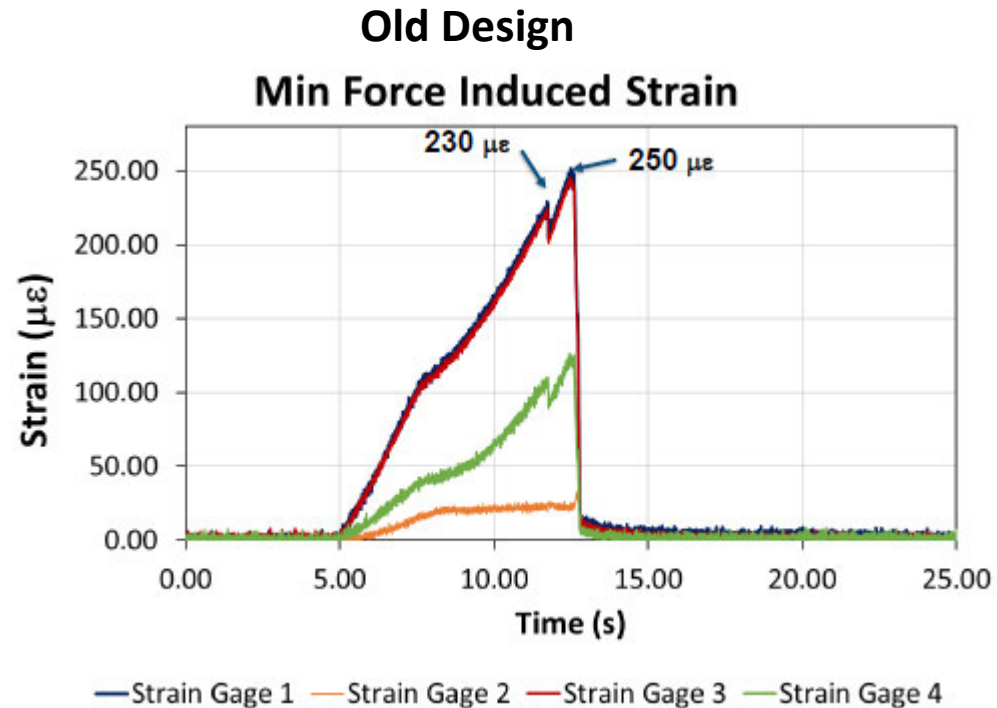


Maximum Principle Strain  $\epsilon_P$ , and the Minimum Principle Strain  $\epsilon_Q$ , which can be oriented at any angle  $\theta$  from the gage axes using the following equation:

$$\epsilon_{P,Q} = \frac{\epsilon_1 + \epsilon_3}{2} \pm \frac{1}{\sqrt{2}} \sqrt{(\epsilon_1 - \epsilon_2)^2 + (\epsilon_2 - \epsilon_3)^2}$$

Maximum Principle Strain  $\epsilon_P$  was used in all experiments shown in results chart

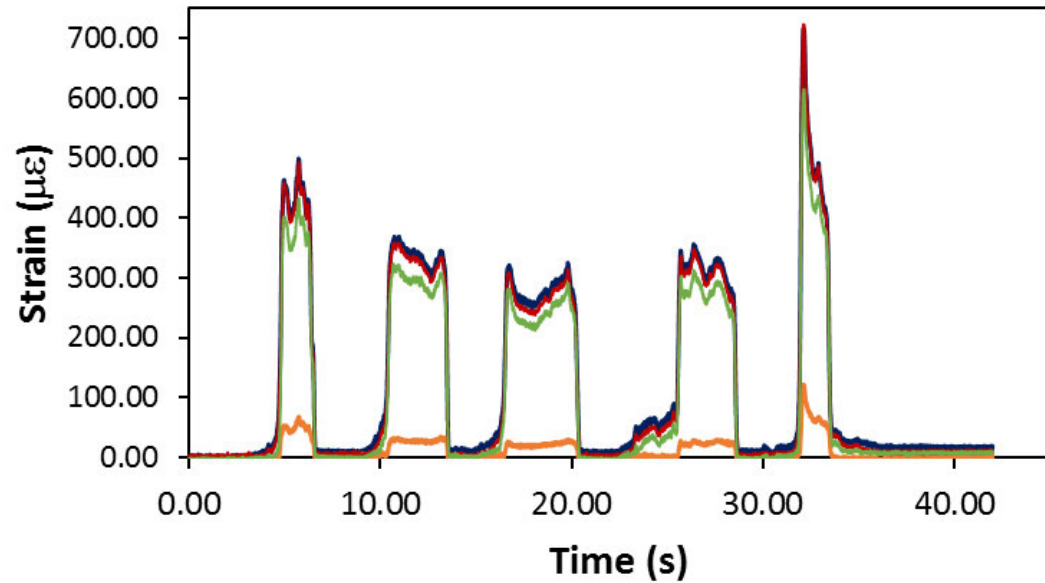
## Part II Results – Minimum Load to Activate Button



- The first peak load is the minimum load to activate the button
- The second peak load is the load at the push stop point, where the button was pushed after activation

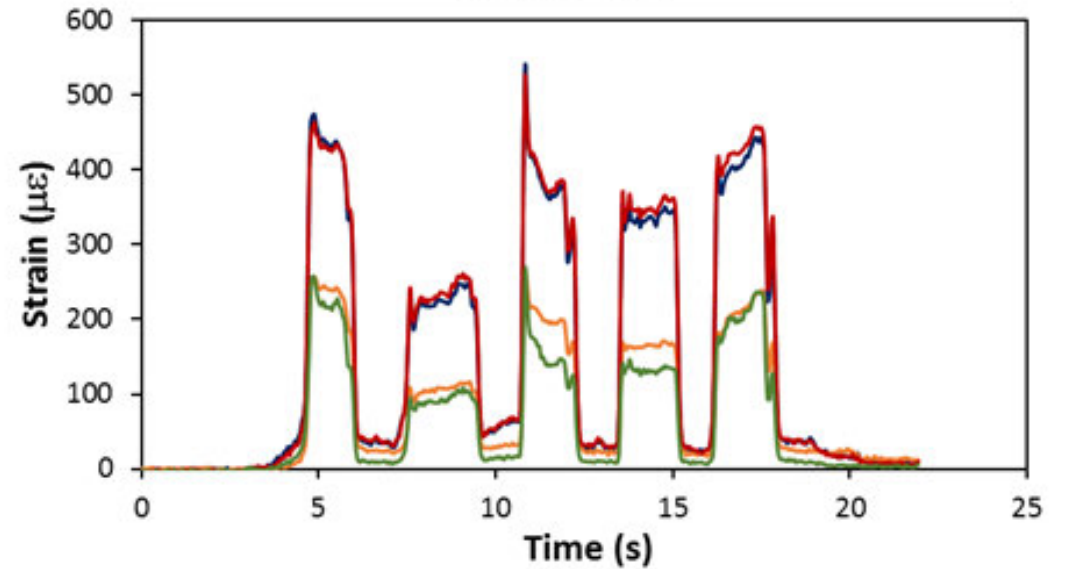
## Part II Results – Human Operating Tests

Old Design



— Strain Gage 1 — Strain Gage 2 — Strain Gage 3 — Strain Gage 4

New Design



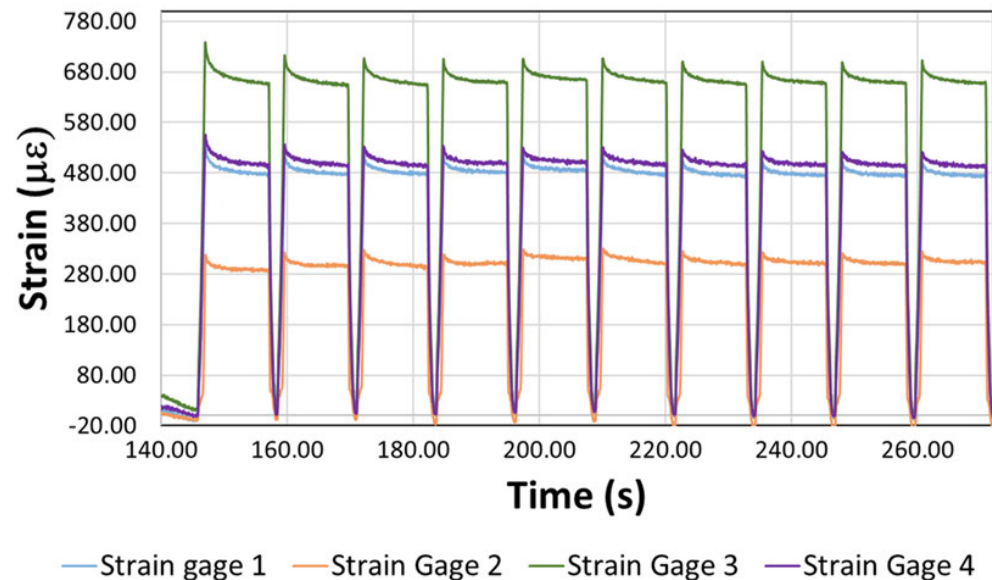
— Strain Gage 1 — Strain Gage 2 — Strain Gage 3 — Strain Gage 4

- The max strain for old design is about 700  $\mu\epsilon$ , average strain is 432  $\mu\epsilon$
- The max strain for new design is about 500  $\mu\epsilon$ , average strain is 362  $\mu\epsilon$
- Both max strain and average strain were reduced in the new design

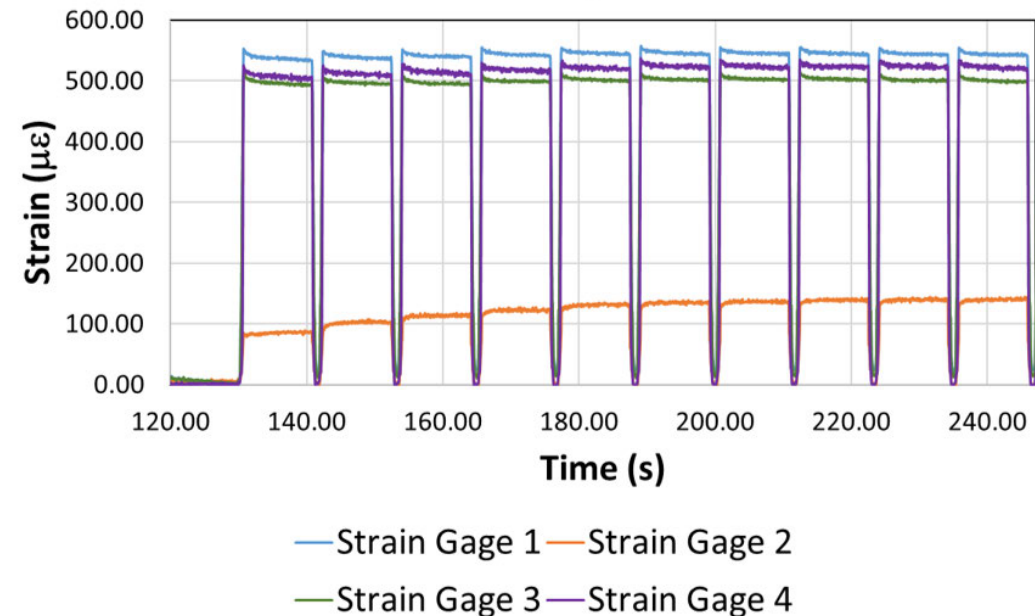
## Part II Results – Machine Controlled Push Test

- Maximum strain found from human operating tests were used for machine button push tests
- Tests were stopped at 40,000 cycles, equivalent to 3 months' usage time

Old Design Tests

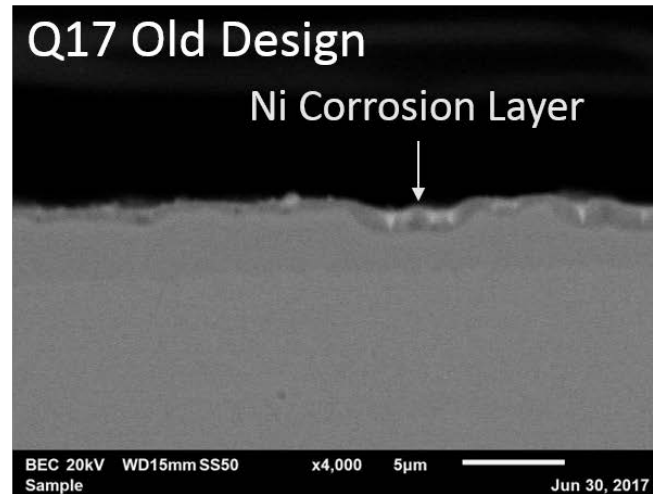
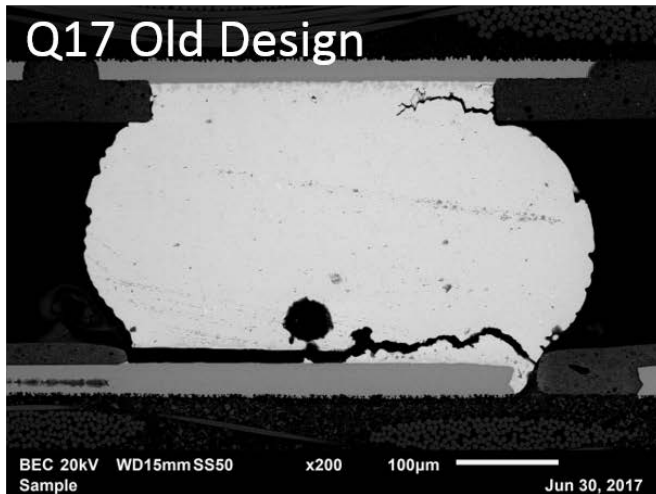
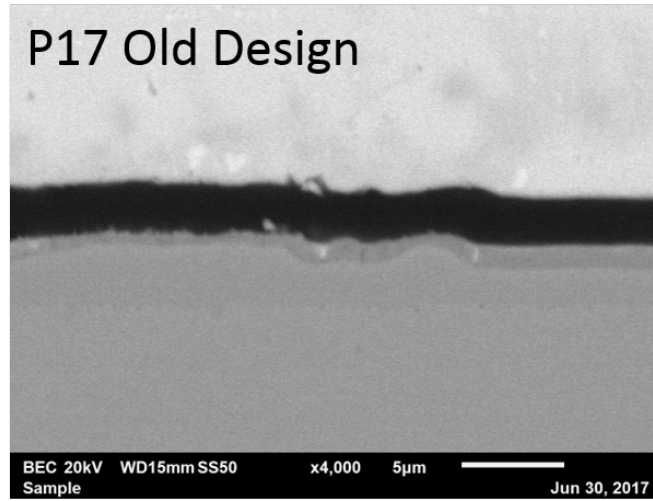
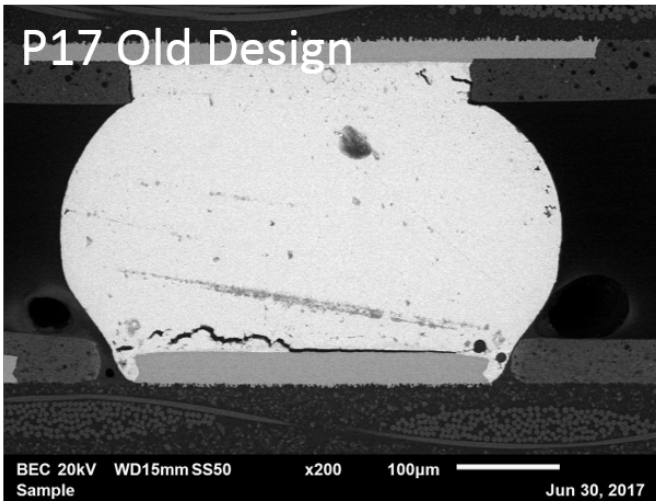


New Design Tests



- Only the first 10 cycles were shown in the plots, similar strain levels after 10 cycles were obtained
- Strain gage 3 shows highest strain in the old design of 700  $\mu\epsilon$
- Strain gage 1, 3, and 4 shows similar highest level of strain of 500-550  $\mu\epsilon$  in the new design

## Part II Results – Failure Mode in Old Design

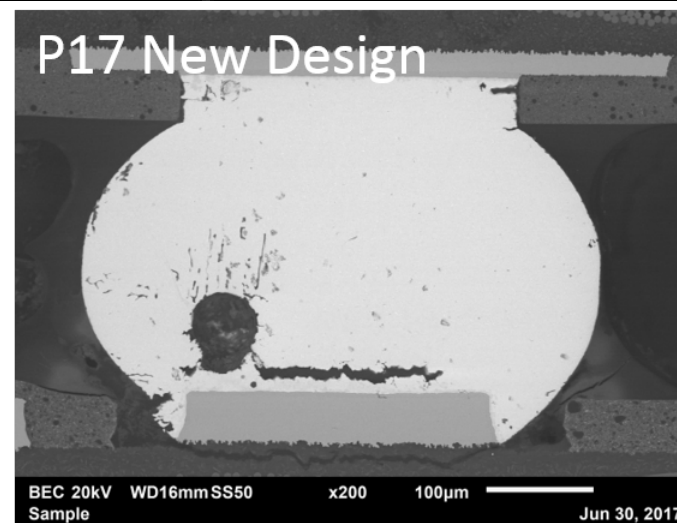
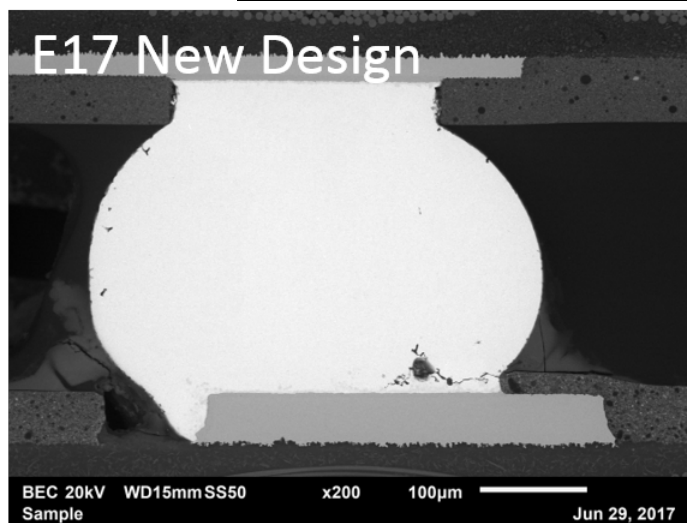
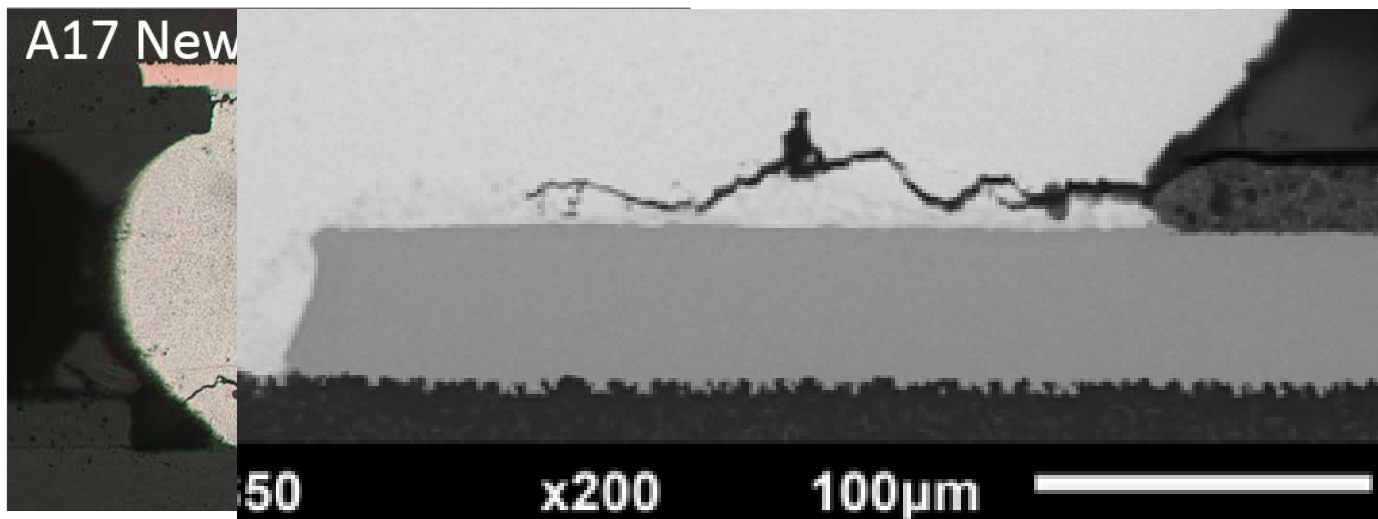


### Failure Modes:

- P17 and Q17 shows similar failure modes with a mixture of brittle fracture at IMC/Cu pad interface, and ductile cracks inside bulk solder
- The brittle cracks were thought to be first formed at early stage of the cyclic button push tests, and the ductile cracks were later formed at longer cycles of button push tests.
- Cracks tend to initiate at the edge of the pad that connect to trace lines, which are thought to be the high stress concentrations in these regions.

**Impact Factors:** strain rate, loading angle, and the IMC layer roughness.

## Part II Results – Failure Mode in New Design



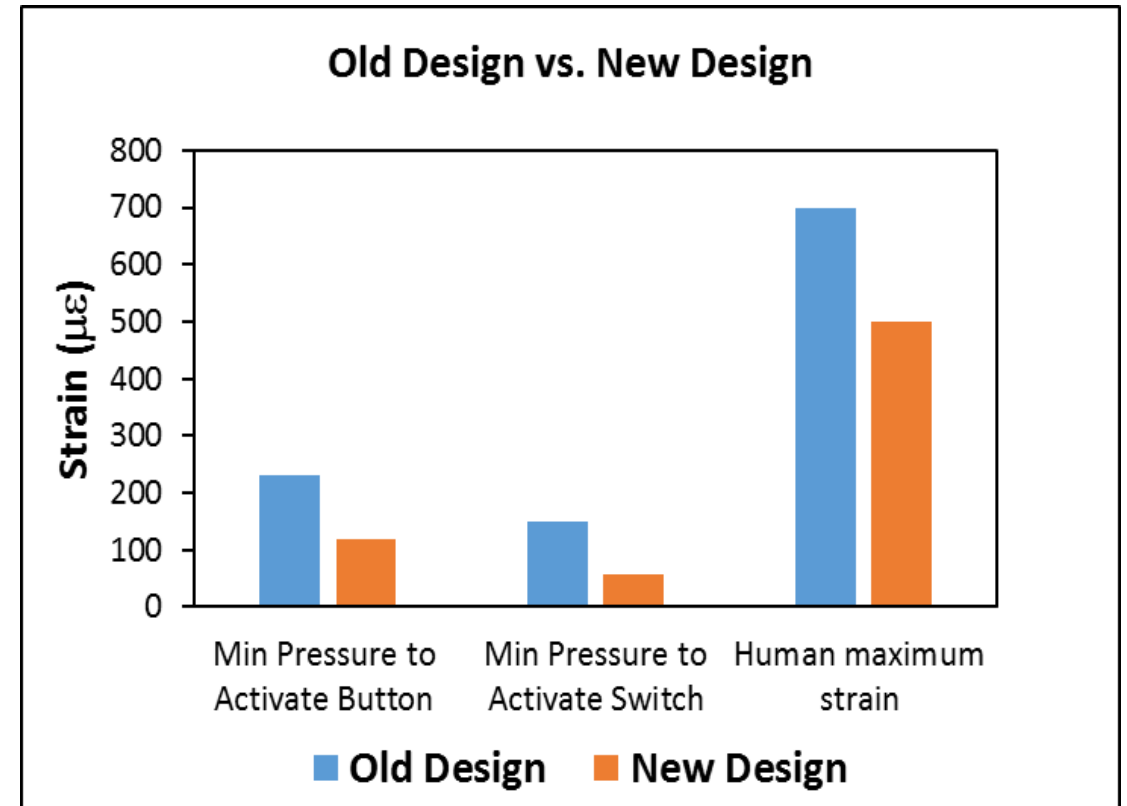
### Failure Modes:

- A17 shows a mixture of brittle fracture at IMC/Cu pad interface, and ductile cracks inside bulk solder
- B17: Crack in the IMC on board side
- E17: Crack initiates from the edge and propagates into bulk solder
- P17: Crack initiates and propagates inside bulk solder

**Impact Factors:** strain rate, loading angle, and the IMC layer roughness.

## Part III – Design Improvement and Results

- **Two Structures**
  - Old Design: rubber button
  - New Design: plastic button, different shape
- **Three Loading Conditions**
  - Minimum pressure to activate the button
  - Minimum pressure to activate the switch
  - Human operated pressure
- **Summary**
  - The minimum pressure to activate the button, switch, and human operated pressure are all lower in the new design
  - Improvement was obtained with less strain levels in different testing conditions in the new design
  - Further optimization of design is suggested to eliminate the failure



# Conclusions

- **Field Returned Units**

- **Failure mode:** Black Pad failure with brittle cracks developed in the interface between IMC and ENIG surface finish on Cu pad
- **Root Cause:** weak solder/pad interfaces are prone to fracture with high strain-rate events
  - Extensive corrosion of exposed nickel surface
  - Creation of brittle phosphorous-enriched Ni-P thin layer
- **Solution:** improve ENIG process, or use alternative surface finishes

- **Experiments of New Units to Simulate Failures**

- **Failure mode:** strain rate, loading angle and IMC roughness are possible impact factors
  - Mixture of brittle cracks at the solder/pad interfaces and ductile cracks inside bulk solder
  - Ductile Cracks inside bulk solder
  - Ductile Cracks in IMC layer
- **Root Cause:** max. solder joints strain close to strain limits from IPC 7904
- **Solution:** make changes of design to lower BGA strain levels

- **Design Improvement and Results**

- Improvement was obtained with less strain levels in different testing conditions in the new design
- Further optimization of design suggested to eliminate failures

## References

1. P. Tegehall, "Review of the Impact of Intermetallic Layers on the Brittleness of Tin-Lead and Lead-Free Solder Joints", IVF Project Report 06/07, 2007.
2. K. H. Lee, "Identification and prevention of "Black Pad" in Sn/Pb soldering", Circuit World, Vol. 37 Issue: 3, pp.10-15, 2011.
3. K. Zeng, R. Stierman, D. Abbott, et al., "The root cause of black pad failure of solder joints with electroless Ni/Immersion gold plating", JOM 58: 75, 2006.
4. J. Nable, "PCB Surface Finishes: A General Review", SMTnet, June, 2015.
5. IPC/JEDEC-9704, "Printed Wiring Board Strain Gage Test Guideline", 2005
6. M.Meilunas, A. Primavera, and S.O.Dunford, "Reliability and failure analysis of lead-free solder joints", IPC Conference, New Orleans, LA, November 2-3, 2002.
7. P. Kumar, Z. Huang, I. Dutta, "Roles of process and microstructural parameters of mixed mode fracture of Sn-Ag-Cu solder joints under dynamic loading conditions", Proceedings of InterPACK, Paper no. 89205, IEEE/ASME CD-ROM, 2009.

## Acknowledgement

The authors would like to thank all Advanced Engineering Group (AEG) members from the company for valuable discussions and suggestions.

# Appendix

# IPC 9704 Printed Wiring Board Strain Gage Test Guideline

